

IMECE2009-11814

GRAVITY-DRIVEN MICROFLUIDIC CELL SORTER BASED ON HYDRODYNAMIC SWITCHING FOR SMALL-MEDIUM SIZE POPULATIONS OF CELLS

Michael Grad

Columbia University
Department of Mechanical Engineering
New York, NY, USA

Lubomir Smilenov

Columbia University
Center for Radiological Research
New York, NY, USA

David Brenner

Columbia University
Center for Radiological Research
New York, NY, USA

Daniel Attinger

Columbia University
Department of Mechanical Engineering
New York, NY, USA

ABSTRACT

In this work we show the design and characterization of a microfluidic cell sorter. The device is designed to sort small quantities of live cells labeled with either live dyes or Green Fluorescent Protein (GFP). Manually operated, it reaches frequencies of 10 cells per minute. Sorting occurs through hydrodynamic switching, with low hydrodynamic shear stresses, preserving to a high degree the pre-sorted cell status. Also, the cells are not subjected to any electric or magnetic field. The chip is made from reusable hard plastic material (PMMA) into which microchannels are directly milled with a hydraulic diameter of 70 μ m, and one inlet and two outlet reservoirs are drilled through the chip. A syringe pump provides a sheath flow that deflects the cells into either the waste reservoir or collection reservoir, depending on the state of two fast solenoid valves. The cells are maintained in an isotonic buffer throughout the sorting process. The Peclet number in the channel is large, preventing diffusion of cells to the walls for adhesion. Since the channels are sealed with disposable tape, the cell sorter is easy to clean. The cell sorter was successfully used in the framework of a study on the bystander effect occurring during cell irradiation by sorting 30 cells in less than 3 minutes.

INTRODUCTION

Typical cytometry applications deal with the analysis and sorting of $>10^6$ cells, but there is increasing interest in small cell populations (10-100 cells). Progresses in several important areas of molecular biology are linked to single cell analysis.

Single cell gene expression, miRNA expression or DNA sequencing are considered extremely important sources of information reflecting most exact cell mechanisms [1, 2]. Also, extracellular interactions such as those found in the radiation-induced bystander effect may lead to a better understanding of the consequences of low-dose radiation [3]. In all of the above cases, large population-wide analysis may mask the behaviour of individual cells in biological processes where cellular heterogeneity plays a role [1]. Therefore there are many cases where single cells are separated from small populations and analyzed, and in such cases the capability of sorting $>10^6$ cells is unnecessary.

Several methods are currently available to sort single cells, and they differ with respect to the sorting mechanism, the sorting efficiency (or losses) and the sorting frequency (or typical cell amount per batch). The most widely used device for cell sorting of large populations is the flow cytometer, based on Fluorescence Activated Cell Sorting (FACS). Commercially available products are available from companies such as Becton Dickinson, Coulter, Partec, and Union Biometrica, among others [4-6]. These commercial cytometers use either 'droplet deflection' or 'stream switching' to deflect cells into separate reservoirs. In the former case, cells are encapsulated into droplets, their fluorescence is measured, and they are electrostatically or pneumatically deflected into separate reservoirs. In the latter case, a piezoelectric fluidic valve deflects sorted cells down a separate arm than unsorted cells. These products are mostly designed for fast separation of large populations, with typical throughputs ranging from 300 cells/second to over 10 000 cells/second [6]. Cells are typically

fixed, and their application in the sorting of live cells may induce cell stress [7]. This requires subsequent cell recovery where the cell status before the sorting (frequently of great interest to the investigators) is lost. Also traditional flow cytometers are large, expensive instruments difficult to integrate into further processes involving microfluidic chips. It is obvious that applications with small populations of cells (~10-100) are not meant to be sorted in cytometers – they will be lost in the sample volume alone, and it is not necessary to sort with such high throughput of >300 cells/second. Therefore we propose a microfluidic sorter meant to handle single cells from small populations, with the advantage of possible integration into other microfluidic processes.

Single cells can be sorted manually from small populations by a skilled operator using micropipettes, microgrippers or size-based filters [8, 9]. The typical sorting frequency with these methods is very low (~1 cell/min) and the physical manipulation may cause damage to the cell. Also, single cell manipulation can be achieved by integrating microfluidics with magnetic, optical, electrical, or hydrodynamic forces. These microfluidic sorters all have typical sorting frequencies in the Hz regime – between physical sorting and flow cytometry [8-11]. Magnetic manipulation generally relies on attaching magnetic beads to cells in a selective manner; magnetic fields can then be used to manipulate the cells [9]. Optical tweezers can trap a cell or particle by the combination of a gradient force and a scattering force from a gaussian beam. These devices have the advantage of non-contact and contamination free manipulation, but are limited by their expensive equipment and complex optical setups [9]. Electrophoresis uses DC current to move charged particles and Dielectrophoresis (DEP) uses a non-uniform AC electric field to manipulate dielectric materials. The clear advantages of electrophoresis methods are speed, flexibility, controllability and ease of automation, while electric fields may affect the cells [8, 9, 12].

Hydrodynamic cell sorters rely only on hydrodynamic forces to separate cells. A very simple example of an on-chip hydrodynamic cell sorter relies on flowing cells into a Y-connection and selectively blocking with e.g. a valve one outlet port so that cells are forced to the other outlet [13]. A drawback of this scheme is that cells such as fibroblasts might adhere to the channel walls when the flow is turned off. Also, turning off

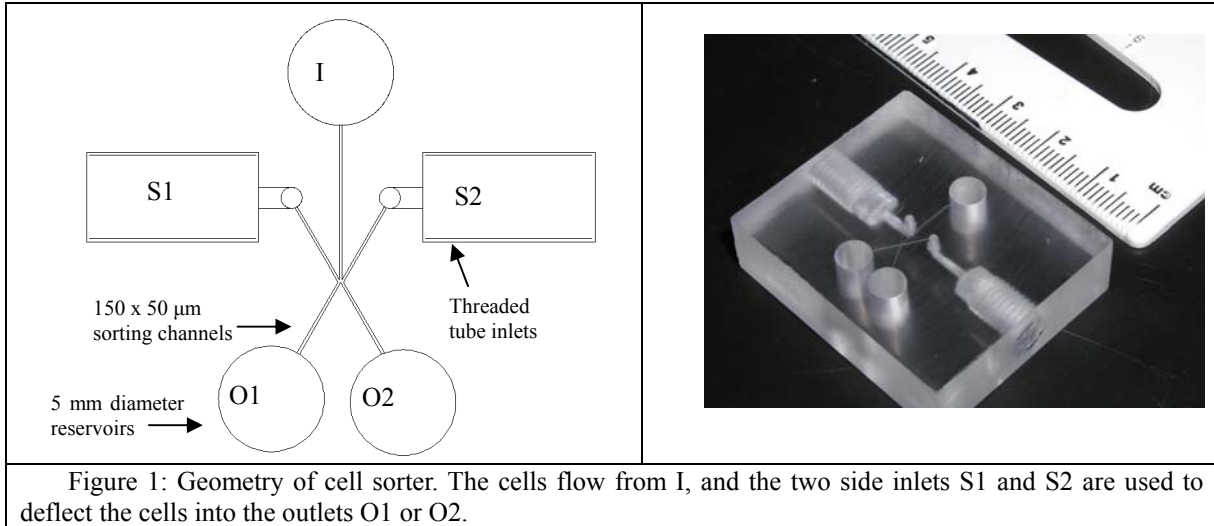
a valve may damage cells passing through it. For these two reasons, more sophisticated hydrodynamic cell sorters have been designed, with the goal to sort small amounts of cells with minimal losses.

Hydrodynamic sorters that do not stop the outlet channel flow have been successfully shown in [14, 15]. Kruger et al. [15] described the development of a hydrodynamic cell sorter coupled with fluorescence detection. Sheath flow driven by syringe pumps was used to direct the flow from the main channel carrying beads to either one of two outlet channels. The flow was controlled by syringe pumps with a relatively long switching time, on the order of 200 milliseconds: this caused backpressure interferences and the authors concluded that their hydrodynamic switching device required more optimization in terms of precise flow control. Later, Dittrich et al. [14] used a X-shaped geometry analog to Kruger et al. [15] to sort cells, where electrokinetic forces drove the sheath flow.

This paper proposes an optimized X-shaped hydrodynamic cell sorter where switching is driven by a sheath flow. Computational Fluid Dynamics is used to assess the performance of the device and the stress exerted on the cells. Channels are milled in a hard plastic chip that can be used several times. In our design, syringe pumps drive the sheath flow so that no electric forces are exerted on the cell. Also, fast solenoid valves with 0.5ms switching time are used to suppress backpressure interference, so that single cells can be individually sorted. Also, we use gravity to drive the main flow containing the cells, between open reservoirs that can be easily accessed by pipette. Finally, the microfluidic channels are sealed with tape, which can easily be removed for cleaning the reusable chip.

CONCEPT AND DESIGN

Figure 1 shows the geometry of the cell sorter. The sorter involves the intersection of three inlet channels S1, S2, and I, and two outlet channels O1 and O2. Gravity drives a cell-loaded solution from the inlet (I) to the cross section. At this point, cells are deflected in either outlet channel by a sheath flow determined by the state of two valves located at S1 and S2, which are reciprocally open or close.



The generation of a hydrostatic pressure with a height difference Δh is chosen to drive the cell flow through the main channel because it allows convenient free access with a pipette to inlets and outlets. To allow enough recognition and reaction time for the operator sorting the cells, the target design cell speed is chosen as $V=0.5$ mm/s. The cross section of the channels was chosen to be $150 \mu\text{m}$ by $50 \mu\text{m}$, about 10 times the cell size so that clogging is prevented, resulting in a hydraulic diameter $D=75 \mu\text{m}$. Assuming the cell solution has the volumic mass of water, $\rho=1000 \text{ kg/m}^3$, and a viscosity of $0.001 \text{ Pa}\cdot\text{s}$, we obtain a Reynolds number $\text{Re} = \rho U D / \mu$ of about 0.035. The flow is therefore clearly laminar with negligible inertial effects, and cells following streamlines without turbulent oscillations. The pressure difference required to drive this flow is given by [16]:

$$\frac{64}{\text{Re}} \frac{L}{D} \frac{1}{2} \rho V^2 = \Delta P = \rho g \Delta h \quad \text{Eq 1}$$

For a travel length in the chip of $L=20\text{mm}$, we need a pressure difference $\Delta P=50 \text{ Pa}$, corresponding to a height difference $\Delta h=5 \text{ mm}$. The heights of the inlet and outlet reservoirs are therefore designed to be at least 10 mm to give more control over the speed of the cells. Figure 2 shows the design and a picture of our cell-sorting chip. The 5 mm diameter reservoirs are clearly shown and allow for access with a pipette. The side channels have threaded holes that allow for standard microfluidic connections to the syringe pump. The entire chip is under $4\text{cm} \times 3\text{cm}$ long.

The target speed was chosen as 0.5 mm/s because this speed is slow enough for manual operation (taking into account human reflexes), and fast enough to prevent cells from adhering to the walls. A possible explanation for cells not adhering to the walls can come from the analysis of the Peclet number:

$$\begin{aligned} \text{Pe} &= LV/D = \text{convection/diffusion} \\ \text{Where } D &= K_B T / 6\pi\eta r \text{ (Einstein)} = 1\text{e-}14 \\ V &= 0.5\text{mm/s} \\ L &= 20 \mu\text{m} \text{ (half channel height)} \end{aligned}$$

The Peclet number is therefore calculated to be $1\text{e}6$. The large Peclet number means convection dominates, and particles do not diffuse to the walls for adhesion.

The sheath flows are driven by a syringe pump and controlled with two micro-solenoid valves (Gyger AG, Switzerland, 0.5 ms switching time). For testing purposes, a push-button electronic switching mechanism controls the reciprocal state of the two valves at S1 and S2, so that an operator can sort cells by visual inspection under a fluorescent microscope. Two light-emitting diodes are included on the controller to show the operator the state of each valve, and a generic AC/DC converter plugged into an AC wall outlet provides the 5V operating voltage. Automation can be easily implemented by controlling the solenoid valves with a computer.

In the design process, we used Computational Fluid Dynamics to determine the maximum operating frequency of the cell sorter, and the maximum shear rate experienced by the cells. The finite-element multiphysics software COMSOL was used to simulate the flow at the intersection of three inlet channels and two outlet channels. A 3D mesh was generated by COMSOL with 10 nodes along the z axis and 200 nodes along the x/y axes, corresponding to XY tetrahedral elements. As a boundary condition, a pressure difference of 50 Pa , corresponding to the above calculation from equation 1, was applied between the inlet and outlet reservoirs. The closed valve was modeled as a wall.

Figure 2a shows the outcome of a steady state flow simulation. In the configuration described, the top left valve is closed while the top right valve is open. The average speed of the flow in the simulation is about 0.8mm/s , in good agreement with the design goal of 0.5mm/s . Trajectories shown in black lines in figure 2a show that the presence of a sheath flow at the right deflects the particle-laden flow towards the left channel. Reciprocally, figure 2f shows that in the opposite valve

configuration deflects the particle-laden flow towards the right channel.

A transient simulation was then performed to calculate the time it takes for the flow to adapt to a sudden change in the valve state. By adapting, we mean that suddenly switching the valves correspond to a sudden change of boundary conditions, creating unsteadiness in the flow until a new steady state is obtained. Figures 2a-2f show a time-sequenced series of images of the switching. The flow switching time from the simulation is about 0.5ms as the flow in the right channel stops and the flow in the left channel starts. The low Reynolds number ensures that no vortices will be created and that the flow will remain laminar. Theory predicts that the switching

time depends on the hydraulic diameter, a , the smallest Bessel function root, γ_1 , and the viscosity of the fluid, μ [17]:

$$t_{acc} = \frac{\rho}{\gamma_1^2} \frac{a^2}{\mu} = 0.97ms$$

The switching time calculated analytically and numerically is therefore on the same order, and corresponds to a theoretical maximum switching (and sorting) frequency of about 1kHz, upon automation of the sorting. This frequency is on the same order to the frequency of the valves that we have chosen (2kHz): this indicates that maximum practical switching frequency of our device will be close to the maximum theoretical switching frequency, as determined by computational fluid mechanics.

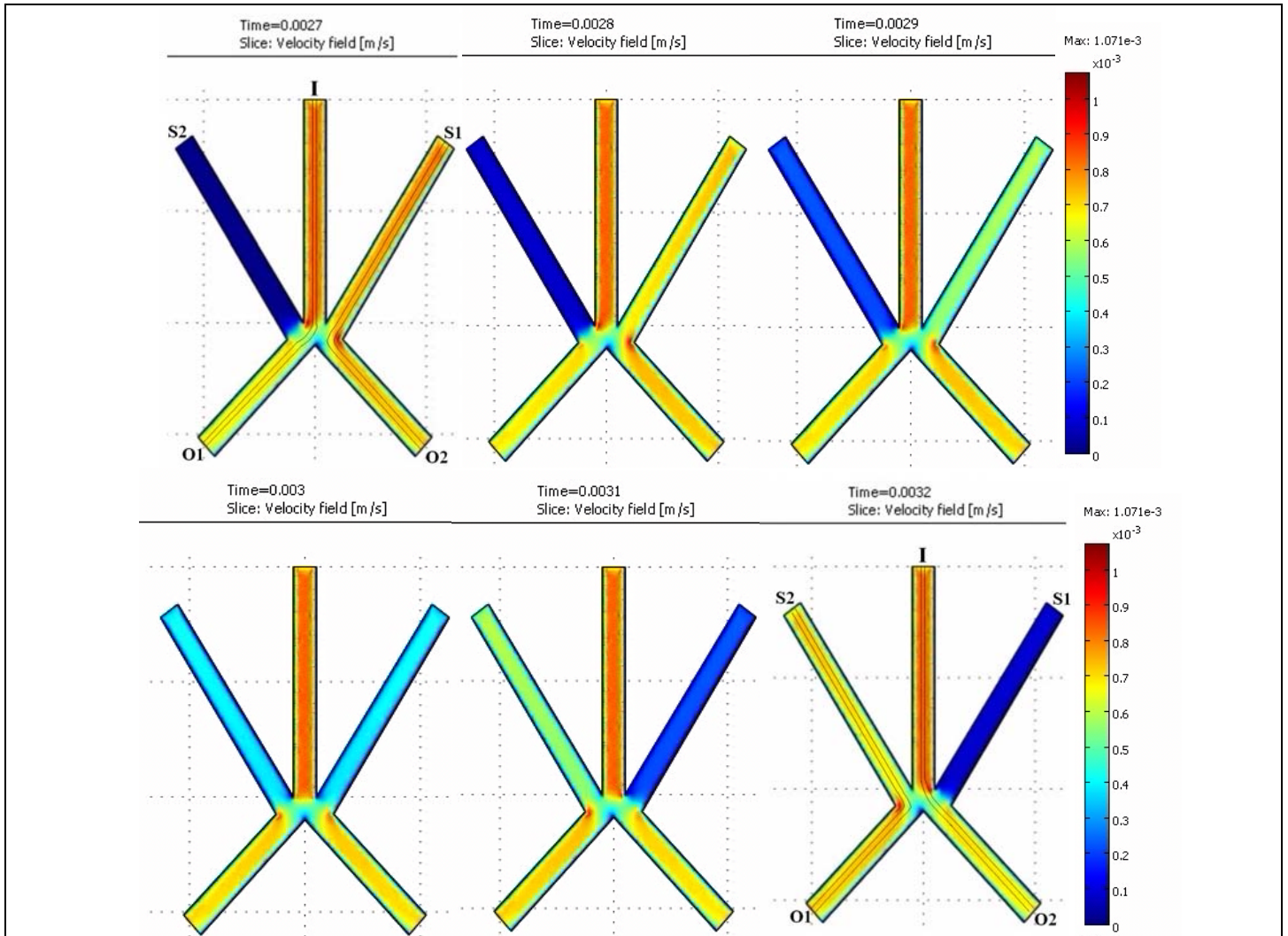


Figure 2: COMSOL simulation showing the velocity magnitude during switching. The total process takes about 0.5ms.

The maximum shear stress experienced by the cells corresponds to the magnitude shear stress on the fluid. The shear stress is defined by [18]

$$\tau = \mu \left(\frac{\partial u_i}{\partial x_j} + \frac{\partial u_j}{\partial x_i} \right)$$

The maximum shear stress was calculated from the computational fluid dynamics simulation results as the matrix 1-norm of the above tensor. We found the maximum stress occurs along the walls, with values of 0.042 Pa. This is on the same order as the analytically-estimated average shear stress [19]:

$$\tau \approx \mu \frac{u}{h/2} \approx 0.02 Pa.$$

Typical damaging shear stresses are above 0.4Pa [19]. We can therefore conclude that our hydrodynamic switching scheme is safe for the cells.

MANUFACTURING

The chip was machined from Poly Methyl Methacrylate (PMMA), a hard transparent biocompatible plastic, using a CNC milling machine (Fidal VMC, USA) and 100um end mill (Dixi Inc, Switzerland). The channels were milled directly into the chip, and the inlet and outlet reservoirs were drilled perpendicular to the chip with a 5mm drill bit. The tube connections were drilled and threaded from the side so that standard microfluidic connections could be used (Upchurch Scientific, USA). The channels are sealed with a transparent self-adhesive tape (Adhesives Research, USA), which can be easily replaced while cleaning the channels. Our cell sorter can therefore be reused as many times as necessary.

OPERATION AND RESULTS

The microfluidic chip described here was used for separation of cells expressing GFP or stained with vital dyes from non-stained cells in a scenario typical for bystander effect experiments, where fluorescent cells are plated together with non-stained cells and irradiated with a microbeam [16]. An essential step in these types of experiments is the precise separation of the irradiated cells from the non-irradiated cells for subsequent cell analysis. The peripherals required to operate the chip include a fluorescence microscope so that the operator sees the cells and decides in what bin they should be sorted, and a syringe pump.

To prevent clogging by e.g. undesired air bubbles, the channels and chambers are initially primed with isotonic buffer (filtered Isotone, Becton Dickinson, NJ). Most Isotone is then carefully removed from each chamber, leaving an equal amount of 50 μ l of fluid per chamber, corresponding to a height of \sim 2 mm. The reason for not leaving the outlets empty is that Laplace forces generated by menisci in the small channels might overcome gravity and stop the flow.

At this point one the syringe pump is started, initiating a flow that would direct all cells to one of the outlet chambers (usually the chamber that will act as the “waste” chamber).

Once sorting starts, the cells of interest could be directed to the other chamber, designated as “collection” chamber, by pressing the controller’s button.

Two sorting procedures were used during our utilization of the cell sorter: (a) both types of cells are tagged with different colors of fluorescence, or (b) only the irradiated cells are tagged. In the first case, the irradiated cells are labeled with fluorescent nuclear dye (Hoechst 33342) or GFP, and the bystanders are labeled with vital cytoplasmic dye Cell Tracker Orange, and both can be visualized with a double-pass filter. In the second case, only the irradiated nuclei are tagged and sorted from the non-labeled cells. This method ensures that the tagging does not affect the results from the subsequent analysis, and is fully described below.

Normal human fibroblasts (AG01522 cells) expressing GFP or stained with Cell Tracker Green (Molecular probes, Eugene, OR) were plated in ratio of 1:3 with non-stained cells. After 24 hours the cells were trypsinized, washed and resuspended in Isotone to eliminate small particles that are usually present in unfiltered media. A 100 μ l suspension of cells with concentration of 20 cells/ μ l was placed in the inlet reservoir, mixed by pipetting. This initiated a cell flow at a velocity of about 0.5mm/s. Cells reached the sorting zone at a rate of about 1 cell every 10 seconds, and were observed by the operator under the fluorescence microscope by using a combination of filtered fluorescent light (FITC filter) and visual broadband light allowing the user to simultaneously see both fluorescent and non stained cells.

At this stage all cells were driven to the waste chamber by the default state of the controller. Once it was clear that there is a constant flow of cells, the white light was dimmed and cell sorting was performed only under fluorescent light. By pressing the button all non-fluorescent cells, even if not visible, were directed toward the collection chamber. All fluorescent cells once they appeared in the field of view were directed to the waste chamber by releasing the controller’s button. Using a magnification of 4x gives the operator at least 3 seconds to see the fluorescent cells before they reach the cross section of the channels, allowing for their reaction time and ensuring error free sorting. By operating the chip under only fluorescent light, it is possible to even sort cells with very low levels of fluorescence which might be the case for GFP expressing cells.

It is important to note that successful use of this method ensures that the collection chamber will contain only the non-stained cells of interest, while the waste chamber might contain some non-stained cells, together with the discarded stained cells.

Using this process it was found that about 30 cells could consistently be sorted, without error, and in less than 3 minutes. The turnaround time between tests was under 2 minutes, corresponding to the time to pipette the chambers and re-prime the channels. Three snapshots of the sorting process can be seen in figure 4, where three snapshots of the sorting are taken under white light to visualize the chip channels: an incoming cell, and a cell directed into each channel.

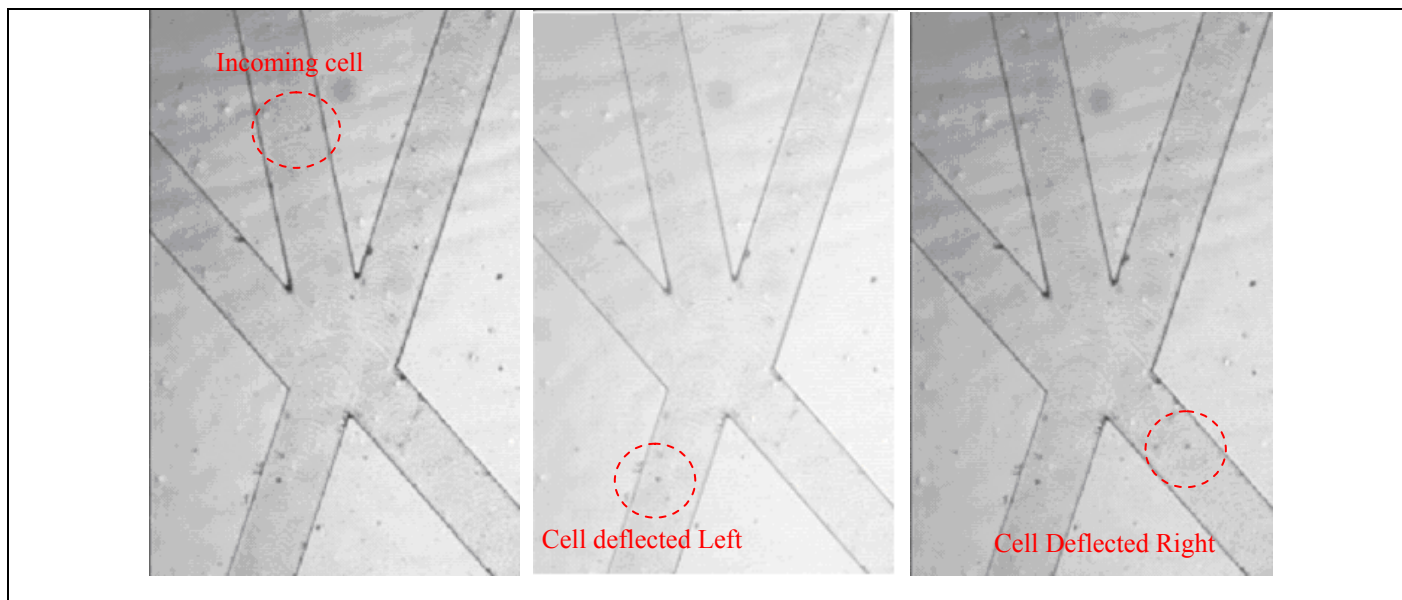


Figure 4- pictures of sorting cells without fluorescence. Every second cell was deflected in the opposite direction. Background dots are from the tape, and are less noticeable in the associated movie.

The above experiments are performed by manually operating the solenoid valves with a pushbuttons switch. As a result, the sorting frequency is low (~10 cells/min), but is sufficient for small populations of cells and to prove the concept of this device. The low frequency of sorting is caused by the large distance between cells to allow extra time for the operator's reaction reflexes. Automating the detection and sorting will eliminate this requirement for this reaction time and allow much higher throughputs. The maximum theoretical throughput (if sorting were limited by the hydrodynamics alone) is ~1kHz due to the time it takes for the pressure to equalize in the channel. Automation will also lead to decreased operational costs for large populations of cells, as an operator will not be required to perform the sorting.

CONCLUSION

A hydrodynamic cell sorter was designed, manufactured and tested for cell sorting in very mild conditions ensuring minimal cell stress. The cells never stop flowing through the device, reducing the risk of cell adhesion to the surface. The inlet and outlet chambers are easily accessed by pipette, and the main cell flow is driven by gravity. Computational fluid mechanics has been shown to be a useful tool to assist the design and predict device performance. The actuation scheme depends on a syringe pump and two microsolenoid valves. Operating only under fluorescent light allowed reliable separation of cells even with low fluorescent intensity from non-fluorescent cells. Finally, the sorter was tested to flawlessly sort 30 cells in less than 3 minutes.

ACKNOWLEDGMENTS

This work was supported by U19 AI067773, the Center for High-Throughput Minimally Invasive Radiation Biodosimetry, from the NIH/NIAID and NIH grant 5P41EB002033.

REFERENCES

1. Longo, D. and J. Hasty, *Dynamics of single-cell gene expression*. Molecular Systems Biology, 2006. **2**.
2. Lu, J., G. Getz, E.A. Miska, E. Alvarez-Saavedra, J. Lamb, D. Peck, A. Sweet-Cordero, B.L. Ebert, R.H. Mak, A.A. Ferrando, J.R. Downing, T. Jacks, H.R. Horvitz, and T.R. Golub, *MicroRNA expression profiles classify human cancers*. Nature, 2005. **435**(7043): p. 834-838.
3. Hei, T.K., H. Zhou, V.N. Ivanov, M. Hong, H.B. Lieberman, D.J. Brenner, S.A. Amundson, and C.R. Geard, *Mechanism of radiation-induced bystander effects: A unifying model*. Journal of Pharmacy and Pharmacology, 2008. **60**(8): p. 943-950.
4. Berthier, J., Silberzan, P., *Microfluidics for Biotechnology*. 2006, Norwood, MA: Artech House, Inc.
5. Watson, J., *Introduction to Flow Cytometry*. 1991, Cambridge: Cambridge University Press.
6. Fisher, D., Francis, G., Rickwood, D., *Cell Separation: A Practical Approach*. 1998, New York: Oxford University Press.

7. Geens, M., H. Van de Velde, G. De Block, E. Goossens, A. Van Steirteghem, and H. Tournaye, *The efficiency of magnetic-activated cell sorting and fluorescence-activated cell sorting in the decontamination of testicular cell suspensions in cancer patients*. Human reproduction (Oxford, England), 2007. **22**(3): p. 733-742.
8. Andersson, H. and A. Van den Berg, *Microfluidic devices for cellomics: A review*. Sensors and Actuators, B: Chemical, 2003. **92**(3): p. 315-325.
9. Yi, C., C.W. Li, S. Ji, and M. Yang, *Microfluidics technology for manipulation and analysis of biological cells*. Analytica Chimica Acta, 2006. **560**(1-2): p. 1-23.
10. Huh, D., W. Gu, Y. Kamotani, J.B. Grotberg, and S. Takayama, *Microfluidics for flow cytometric analysis of cells and particles*. Physiological Measurement, 2005. **26**(3).
11. Voldman, J., *Engineered systems for the physical manipulation of single cells*. Current Opinion in Biotechnology, 2006. **17**(5): p. 532-537.
12. Takahashi, K., A. Hattori, I. Suzuki, T. Ichiki, and K. Yasuda, *Non-destructive on-chip cell sorting system with real-time microscopic image processing*. Journal of Nanobiotechnology, 2004. **2**.
13. Fu, A.Y., H.P. Chou, C. Spence, F.H. Arnold, and S.R. Quake, *An integrated microfabricated cell sorter*. Analytical Chemistry, 2002. **74**(11): p. 2451-2457.
14. Dittrich, P.S. and P. Schuille, *An Integrated Microfluidic System for Reaction, High-Sensitivity Detection, and Sorting of Fluorescent Cells and Particles*. Analytical Chemistry, 2003. **75**(21): p. 5767-5774.
15. Kruger, J., K. Singh, A. O'Neill, C. Jackson, A. Morrison, and P. O'Brein, *Development of a microfluidic device for fluorescence activated cell sorting*. Journal of Micromechanics and Microengineering, 2002. **12**(4): p. 486-494.
16. White, F., *Fluid Mechanics*. 6th ed. 2008, New York: McGraw-Hill.
17. Bruus, H., *Theoretical Microfluidics*. 2008, New York: Oxford University Press.
18. Aris, R., *Vectors, Tensors, and the Basic Equations of Fluid Mechanics*. 1962, Englewood Cliffs, NJ: Prentice-Hall.
19. Wan, J., W.D. Ristenpart, and H.A. Stone, *Dynamics of shear-induced ATP release from red blood cells*. Proceedings of the National Academy of Sciences of the United States of America, 2008. **105**(43): p. 16432-16437.